JOURNAL OF MATERIALS SCIENCE 27 (1992) 1421 - 1427

Monitoring hydrogen embrittlement cracking using acoustic emission technique

A. K. BHATTACHARYA*, N. PARIDA, P. C. GOPE
Materials Evaluation Division, National Metallurgical Laboratory, Jamshedpur 831 007, India

Acoustic emission during delayed failure of hydrogen-charged low-alloy high-strength steel has been investigated. Tests were carried out at room temperature using standard ASTM three-point bend specimens. It was found that the cumulative acoustic emission counts rose slowly in discrete steps with increasing time in the initial stage of the embrittlement process, whereas it rose rapidly in the later stage prior to fracture. It was also observed that the initial embrittlement phase consisting of microcrack nucleation is characterized by low-amplitude (35–55 dB) signals only, whereas the rapid crack growth region is marked with high-amplitude (60–100 dB) signals. These observations indicate that such a change in the pattern of cumulative counts together with the level of amplitudes of the generated signals can be used to detect the so called "incubation period" for hydrogen embrittlement. This kind of early detection of critical cracks may help towards better fracture control.

1. Introduction

It is generally accepted that hydrogen embrittlement involves the initiation and propagation of cracks under the condition of relatively slow strain rate or sustained load, controlled by the diffusion of hydrogen. Time for crack initiation and propagation become highly significant for a structure and the fracture time has been measured over a range of applied stresses and temperatures [1]. The kinetics of the crack initiation and propagation can be indirectly followed by measuring the changes of the electrical resistance [2]. However, because of its low sensitivity, this technique cannot measure the resistance change for a very small crack and also it does not give a detailed insight into the process of crack initiation and propagation.

On the other hand, acoustic waves, as a result of stress corrosion cracking has been shown to provide information on the crack growth process in greater detail than otherwise available [3, 4]. Hartbower *et al.* [4] monitored crack initiation and propagation in weldments and stress corrosion cracking of maraging steel. Their results are correlated more or less exclusively with the cumulative counts of the emitted acoustic signals. Dunegan and Tetelman [5] have also used this technique to monitor the onset of unstable failure of hydrogen-charged linear compliance fracture specimens and also bolts under constant load, both made of AISI 4340 steel, and proposed a power-law relationship between count rate, dN/dt, and stress intensity factor, K. Although they have suggested a critical acoustic emission rate at the onset of rapid fracture, it is necessary to have prior knowledge of the threshold stress intensity for no acoustic emission (AE) or crack growth, to determine this critical value and this somewhat limits its usefulness as a criterion to predict failure. Moreover, their criterion is for the onset of rapid fracture, after which relatively little time is usually seen by the specimen before final fracture. This again limits the applicability of this criterion in a real situation due to lack of available time between the onset of rapid fracture process and the final disintegration of the structure. Gerberich and Hartbower [6] observed high-amplitude AE signals in hydrogen-induced crack growth.

During the past decade, quite a few studies on hydrogen-induced cracking in steel have been made by using AE technique. Dedhia and Wood [7] monitored cumulative counts, events and amplitude distribution and have correlated fracture by the average counts per event data for AISI 4340 steel. Nozne and Kishi [8] concluded that the main source from hydrogen embrittlement of 4340 steel is from the microscopic intergranular fracture because they found that the cumulative AE event count is proportional to the number of intergranular microcracks during stable crack growth. With regard to the effect of hydrogen charging on the embrittlement process in carbon steel, Hieple and Carpenter [9] found a correlation between AE activity and the embrittlement process. None of these studies, however, addresses the hydrogen embrittlement process with particular emphasis on "incubation" under a constant load condition.

The main objective of the present investigation has been to monitor the incubation time to nucleate microcracks in terms of some directly observable AE parameters. Success in monitoring incubation time can be of great help in a real structure susceptible to

* *Present address*: Material Science and Technology Division, Los Alamos National Laboratory, Los Alamos, NM 87545, USA.

hydrogen embrittlement because a relatively much longer time is spent by the structure between incubation time and the final fracture and hence available time in hand for fracture control can be substantial.

2. Experimental procedure

The specimens were made of low-alloy high-strength steel with the composition shown in Table I.

This material was heat treated to obtain an ultimate tensile strength (UTS) value of 1350 MPa ($R_c = 41$) after which ASTM standard three-point bend specimens were made as shown in Fig. 1. They were then cathodically charged with hydrogen in an electrolyte of 1 N H_2SO_4 and 5 p.p.m. sodium arsenite at a current density of 5 mA cm^{-2} for 5 min. After charging, the specimens were cadmium coated and then baked at 150 °C for 30 min. Tests were carried out at constant load level of 80% notch strength and AE signals were monitored throughout the test period.

The equipment used to monitor AE in these tests was a Dunegan 8000 system and a schematic block diagram of the whole experimental arrangement is shown in Fig. 2. The signals from PZT transducer were amplified to a level of 40 dB using a preamplifier (Model 1801-190 B). These were then band-pass filtered between 100 and 350 kHz and then fed into the DC 8000 system. The results were directly produced on a printer attached to the computer system.

3. Results and discussion

Fig. 3 shows the summary of AE signals during the whole period of a constant load test where the load level was set at 80% of the specimen notch strength. It is seen that during testing a total number of 156 active events with 12 132 counts were recorded. For the purpose of analysis, the total period up to failure has also been divided into five distinctly different regions in the plot, in terms of acoustic activity and have been denoted as regions O–A, A–B, B–C, C–D and D–E. Figs 4–7 summarize the AE signals for the regions O–D, O–C, O–B and O–A, respectively, so that one can observe the nature of the generated signals more closely. In all these figures (Figs 3–7) the total event histogram, total count versus time and amplitude distribution, are shown.

TABLE I Elemental analysis (wt %)

C	Mn	Mo	Cr	Ni	Si	P	S	Fe
0.28	1.20	0.12	0.83	1.99	0.52	0.027	0.03	bal.

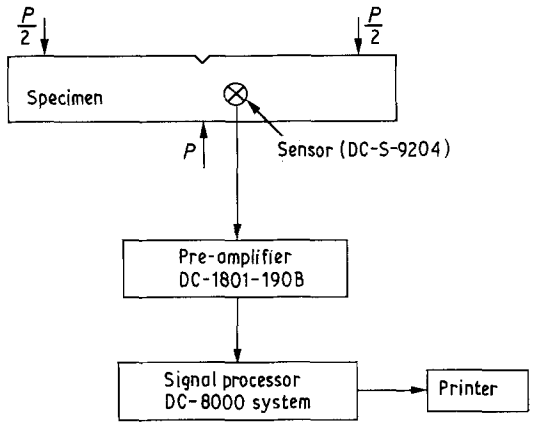

Figure 2 Schematic illustration of the experimental arrangement.

From these plots it is clearly seen that the number of events rises as time progresses along with a rise in the number of counts. Also it is particularly noticeable that the amplitude level consistently dowels between 35–55 dB for all the activities up to C, after which it keeps on continuously increasing until fracture takes place at E (dB level of up to 95). This indicates that higher and higher amplitude signals are observed after point C.

The above observations indicate that the whole region of count versus time in this test (Test 1) may be considered to consist of three distinct regions, as shown also in Fig. 3: (a) Region I from O–C, (b) Region II from C–D, and (c) Region III from D–E. In Region I, which covers most of the time involved in delayed failure, the cumulative count rises very slowly and discretely with time. Also the time steps are much larger than the later stages. Signal amplitudes in this region are also mostly less than 50 dB, except a very few up to 55 dB. It has been observed by various researchers that the early part of the delayed failure process is governed by diffusion of hydrogen into the region of maximum triaxility [1, 5] until a number of microcracks gradually form around these regions. Region I may be considered to represent this early period of microcrack formation. In Region II, the microvoids formed earlier start to coalesce until eventually they form a crack with a critical size (point D) which is the beginning of rapid unstable fracture. We also observe that as the microvoids start coalescing in Region II, amplitude level starts rising beyond 55 dB and reaches even 72 dB which shows that characteristically there is a distinction between the signals generated in Regions I and II. Another feature to note is that in Region II the count rate remains small as in Region I. In Region III the cumulative count plot rises rapidly with higher

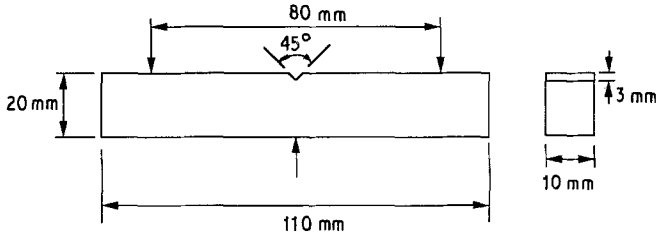

Figure 1 Details of the three-point bend specimen.

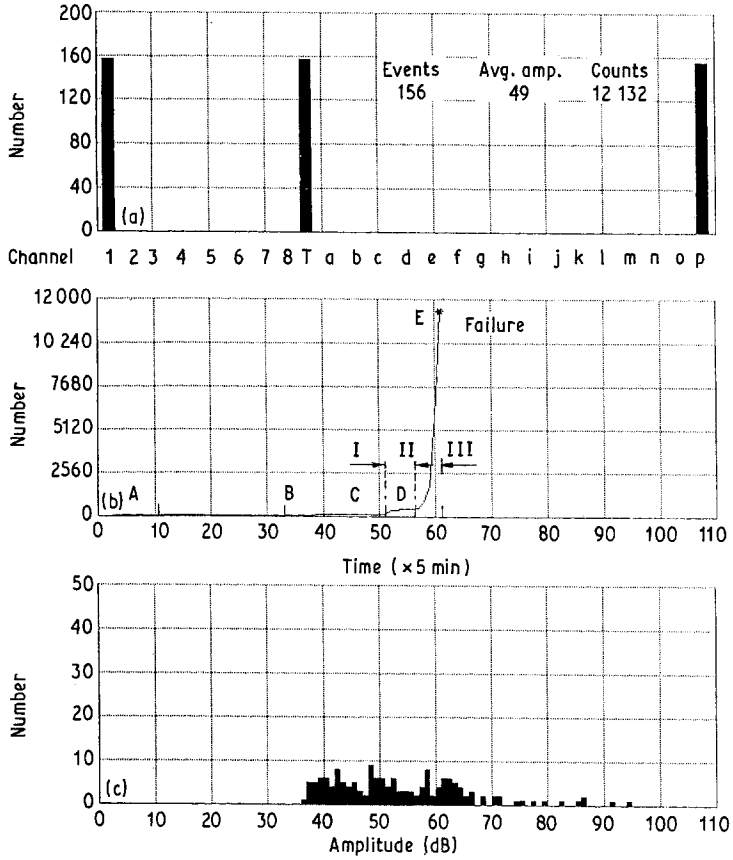

Figure 3 AE activity during the entire period of delayed failure of a specimen loaded at 80% of its notch strength. (a) Total event histogram, (b) total count versus time, (c) amplitude distribution.

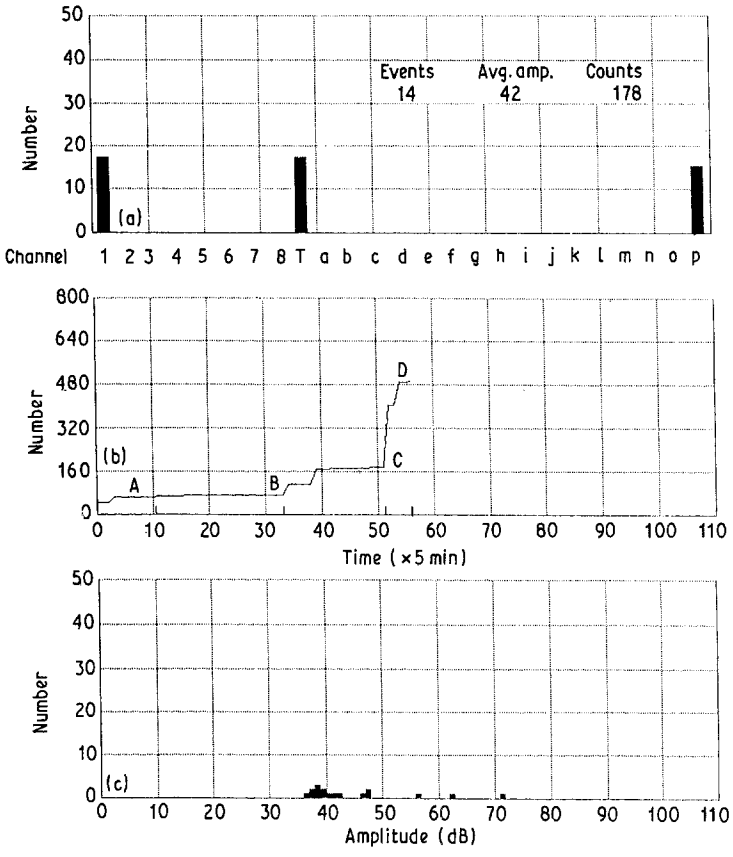

Figure 4 AE activity up to Region D. (a) Total event histogram, (b) total count versus time, (c) amplitude distribution.

count rate and also with higher amplitude signals. In this region the critical crack size nucleated in Region II presumably gives rise to a rapid crack growth and the specimen fails within a short time. Point C may be considered to signify the so called "incubation" of microcracks and point D signifies the nucleation of critical crack which gives rise to rapid crack growth leading to failure.

A number of tests was performed under similar loading conditions, out of which two more typical

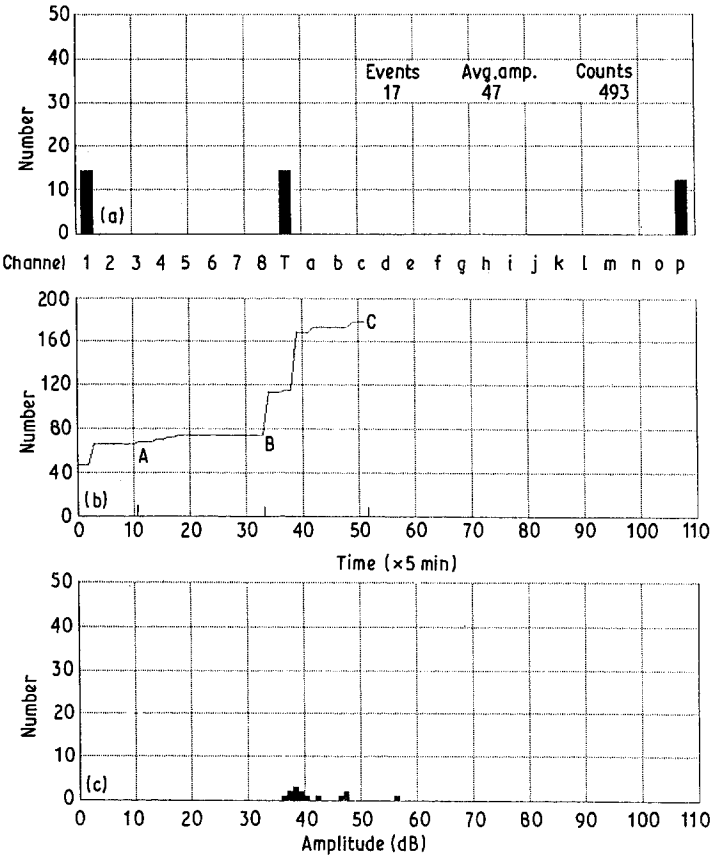

Figure 5 AE activity up to Region C. (a) Total event histogram, (b) total count versus time, (c) amplitude distribution.

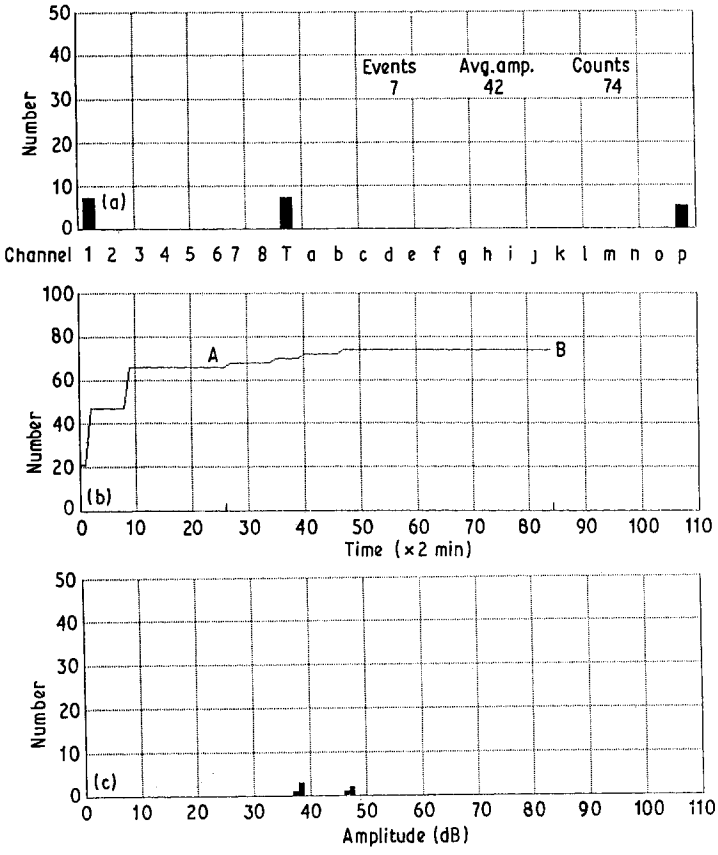

Figure 6 AE activity up to Region **B**. (a) Total event histogram, (b) total count versus time, (c) amplitude distribution.

tests under identical test conditions and loaded at 80% specimen notch strength are also presented. These specimens were machined to have exactly the same geometry as in Fig. 1. The total counts and amplitude distribution after filtering out the undesirable noises are shown in Figs 8 and 9. These plots also show three distinct regimes as before although the shapes and duration are somewhat different. This can be attributed to the statistical nature of hydrogen charging and embrittlement process. But the most

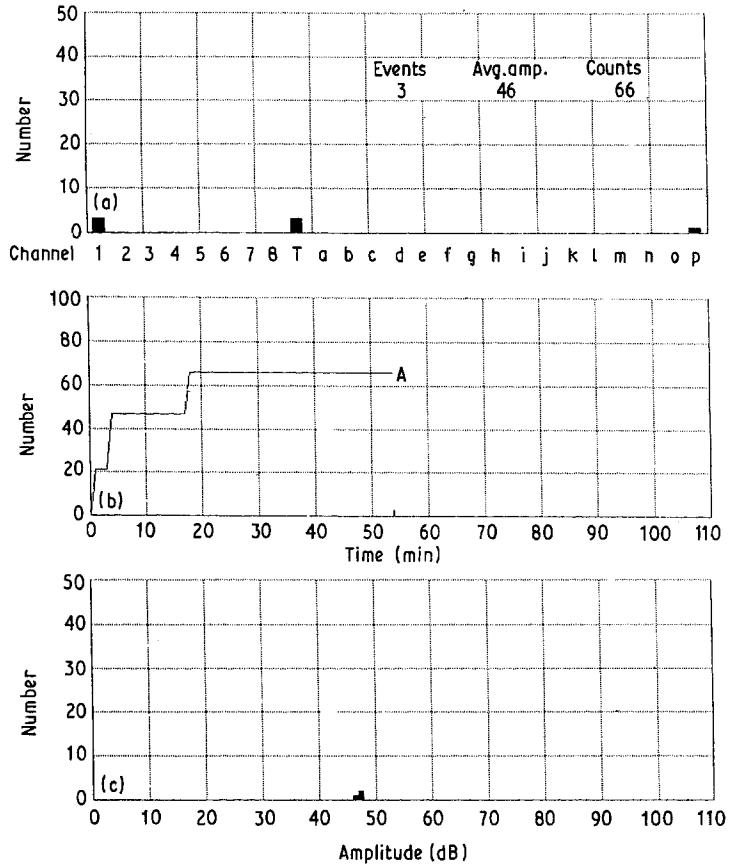

Figure 7 AE activity up to Region A. (a) Total event histogram, (b) total count versus time, (c) amplitude distribution.

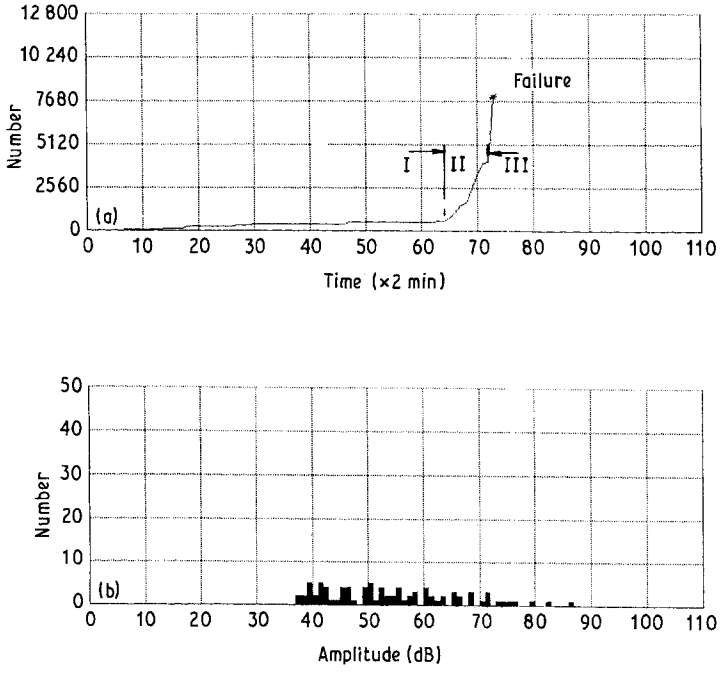

Figure 8 AE activity during the entire period of delayed failure of a specimen loaded at 80% of its notch strength (Test 2). (a) Total count versus time, (b) amplitude distribution.

interesting observation is made when the same kind of signal analysis, as described for Test 1 (Figs 4–7), was also made for Tests 2 and 3. Table II summarizes the range of peak amplitudes in the three regimes covering all three tests. Similarity in the nature of signals is evident in terms of amplitudes.

Fig. 10a and b represent optical micrographs of the fractured three-point bend specimen corresponding to Figs 3 and 9, respectively. As noted earlier, the specimen in Fig. 10a was carried to the final fracture under constant load. The specimen in Fig. 10b was stopped at some point before fracture and broken under cryogenic conditions after being unloaded. The fractured surface in Fig. 10a is seen to be uniformly covered with microcracks. In comparison, the damaging microcracks have extended up to a certain width of the specimen which was unloaded and then fractured cryogenically (Fig. 10b). This clearly signifies that a large number of microcracks form during the embrittlement process, eventually causing fracture. Fig. 10c

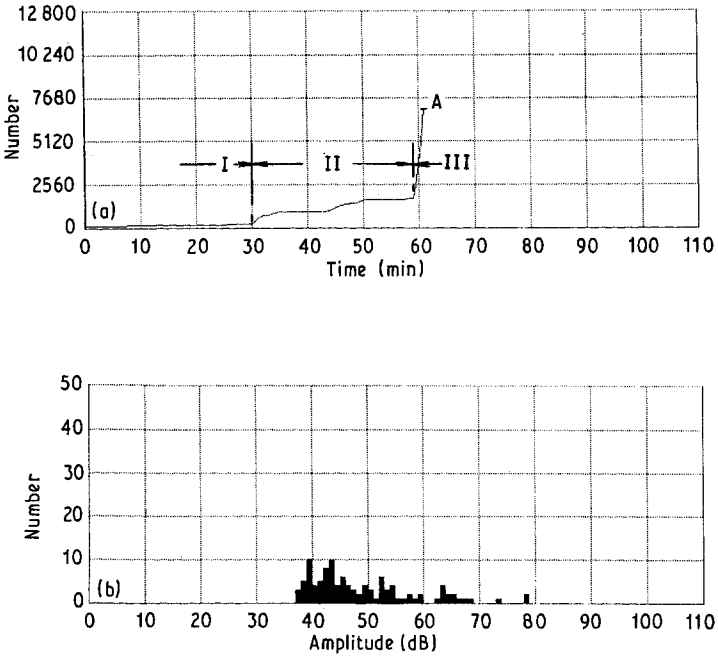

Figure 9 AE activity during the entire period of the embrittlement process of a specimen loaded at 80% of its notch strength (Test 3). Note that the specimen was unloaded at point A for microstructural observation. (a) Total count versus time, (b) amplitude distribution.

TABLE II Peak amplitude of events during the delayed failure of three-point bend specimens loaded at 80% of their notch strength

Test no.	Peak amplitude range of events (dB)		
	Region I	Region II	Region III
1 (Fig. 3)	35–55	50–70	60–95
2 (Fig. 8)	35–60	50–75	70–90
3 (Fig. 9)	35–50	50–70	60–80[a]

[a] Test 3 was not carried to failure but was stopped while in Region III for metallurgical study.

represents a scanning electron micrograph of Area 1 in Fig. 10a which indicates that the cracking mode is intergranular in nature. It also shows that final fracture takes place by ductile separation of ligaments joining the embrittled grains. A few other microcracks perpendicular to the micrographs are also visible. Attempts at direct observation of microcracks just after point C in Fig. 3 are currently in progress.

Thus, if the whole region of a delayed failure is broken up as described for the above tests, a trained operator of a loaded structure under such an environment can usually monitor the count rate and amplitude levels directly through an AE system and predict an impending failure by noticing the change in signal characteristics around point C after which he will have some time in hand to save the structure. The approach taken here is directly monitorable and does not need any further calculation or interpretation. It is also different from a similar approach [5] where a critical count rate was used at the beginning of unstable crack growth (point D in the present case) after which comparatively little time remains in hand to decide the fate of the structure.

It was also observed during these tests that the average rise time of the events is the highest in Region I and decreases towards Region III, whereas the duration of the events in Region I is lowest and increases

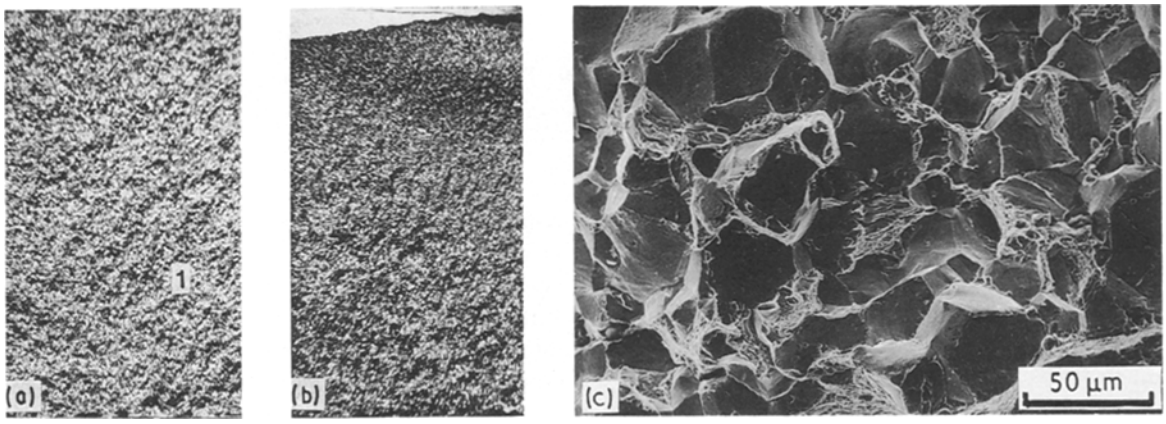

Figure 10 Microstructure of hydrogen-embrittled three-point bend specimen. (a) Optical micrograph of fracture surface by delayed failure, notch side (corresponding to point E in Fig. 3). (b) Optical micrograph of a specimen which was unloaded at point A in Fig. 9 and then cryogenically separated, notch side. (c) Scanning electron micrograph of Area 1 in (a).

towards Region III. This also gives an indication that high-amplitude signals with smaller rise time and longer duration characterize the rapid crack growth period of the brittle failure.

4. Conclusions

1. The beginning of relatively high-amplitude signals together with an increased count rate from the initial low-signal regime can be used as a criterion to signify the incubation of microcracks due to hydrogen embrittlement. This enables one to estimate the so-called 'incubation time' for hydrogen embrittlement.

2. High-amplitude signals with shorter rise time and longer duration are always observed during the rapid growth period. This gives rise to a sharp increase in the acoustic emission rate (of the total count versus time plot) which can be used to monitor the onset of rapid fracture.

3. Microstructural observations provide qualitative agreement between the embrittlement process and acoustic signals.

Acknowledgements

The authors are grateful to Professor S. Banerjee, Director of National Metallurgical Laboratory, for his personal interest and guidance during the investigation and also for permission to publish the results. Helpful discussion with Professor O. N. Mohanty is also appreciated.

References

1. A. R. TROIANO, in "Hydrogen Damage", A Metal Science Source Book, edited by C. D. Beachem (ASM, Metal Park, Ohio, 1977) p. 151.
2. W. J. BARNETT and A. R. TROIANO, *Trans. AIME* **209** (1957) 486.
3. H. H. CHASKELIS, W. H. CULLEN and J. M. KRAFFT, ASTM-STP 559 (American Society for Testing and Materials, Philadelphia, 1974) p. 31.
4. C. E. HARTBOWER, W. G. RENTER, C. F. MORAIS and P. P. CRIMMINS, "Acoustic Emission", ASTM-STP 505 (American Society for Testing and Materials, Philadelphia, 1972) p. 187.
5. H. L. DUNEGAN and A. S. TETELMAN, *Engng Fract. Mech.* **2** (1971) 387.
6. W. W. GERBERICH and C. E. HARTBOWER, in "Conference on Fundamental Aspects of Stress Corrosion Cracking", Ohio State University (National Association of Corrosion Engineering, Houston, Texas, 1969) p. 420.
7. D. D. DEDHIA and W. E. WOOD, *Mater. Sci. Engng* **49**(3) (1981) 263.
8. A. NOZNE and T. KISHI, *J. Acoust. Emission* **1**(1) (1982) 1.
9. C. R. HEIPLE and S. H. CARPENTER, in "Proceedings of DARPA/AFML Review of Progress in Quantitative Nondestructive Evaluation", edited by O. D. Thompson and B. R. Thompson (La Jolla, CA, AFWAL-TR-80-4078, 1979) p. 243.

Received 21 November 1990
and accepted 10 April 1991